

Fig. 2 Current-voltage characteristics measured at various temperatures for different alloy systems: (a) Cd-Sn eutectic, (b) Bi-Sn eutectic, (c) Al-Si eutectic, and (d) Al-3wt.%Si hypoeutectic

ficient of resistivity (α) for each of these alloy systems. We chose alloy systems whose resistivities at 273 K are known. The electrical resistivities of the specimens were calculated from the following equation:

$$\rho = \frac{\Delta V \pi D^2}{4IL}$$

where ρ is the electrical resistivity, D is diameter of the specimen, L is length of the specimen, I is the current, and ΔV is the voltage difference between two probes positioned at a distance of L . The $\Delta V/I$ values obtained from I - V plots.

2. Experimental Procedures

Eutectic (Cd-Sn, Bi-Sn, Al-Si) and hypoeutectic (Al-3wt.%Si) alloys were prepared by melting weighted quantities of >99.9% high-purity Cd, Sn, Bi, Al, and Si in a graphite crucible placed into a vacuum melting furnace (Ref 16). After allowing time for melt homogenization, and then each of the molten alloys was poured into a prepared graphite crucible (200 mm in length, 4 mm ID, and 6.35 mm OD), placed in a hot filling furnace, and then left to cool (Ref 17). After this process, each specimen was removed from its graphite mould.

Thin silver wires (0.05 mm diameter) were then contacted to the ends of the specimens (Fig. 1), and they were fixed using

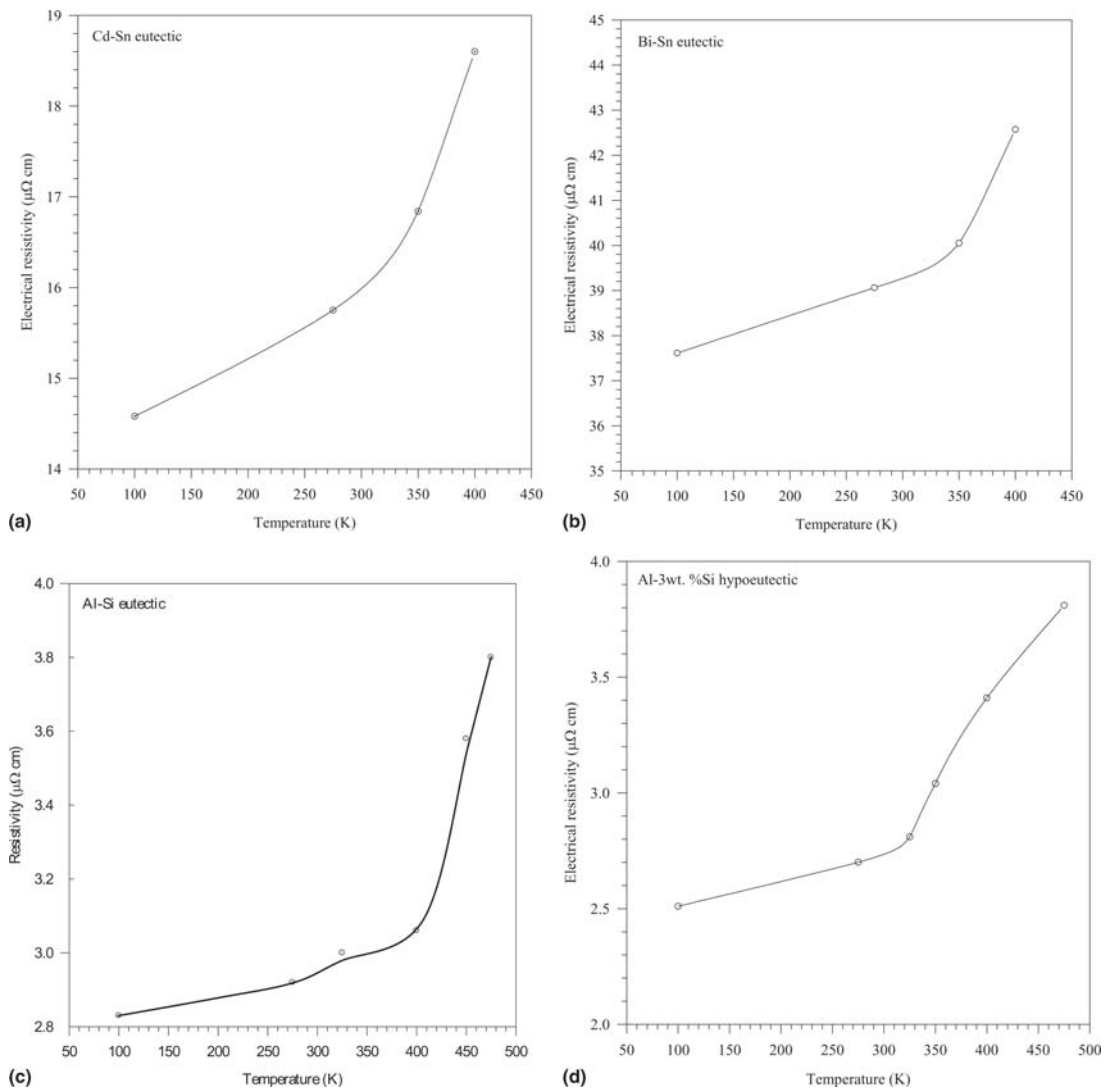


Fig. 3 Electrical resistivity as a function of temperature for different alloy systems: (a) Cd-Sn eutectic, (b) Bi-Sn eutectic, (c) Al-Si eutectic, and (d) Al-3wt.%Si hypoeutectic

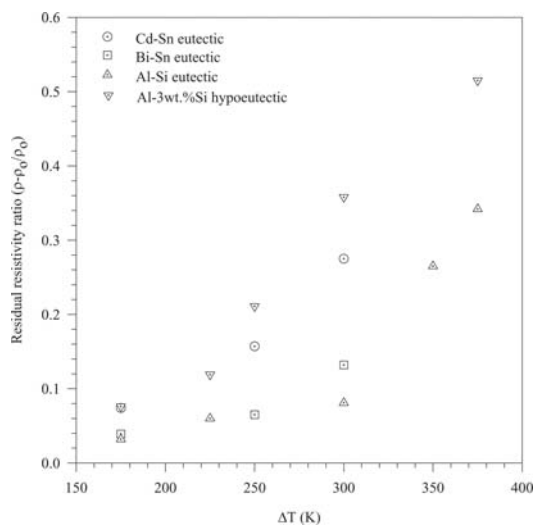


Fig. 4 Variation of the residual resistivity ratio $(\rho - \rho_0/\rho_0)$ as a function of ΔT for different alloy systems

silver paint. Specimens prepared in this way were placed in a horizontal heating furnace on ceramic plates that were aligned horizontally with the specimens. A four-probe direct current (dc) method was used to measure the resistivity.

As can be seen in Fig. 1, the experimental system consists of a horizontal heating furnace, a temperature controller, a Hewlett-Packard (Santa Clara, CA) HP4140B picoammeter (dc voltage source), a plotter, and a computer. *I-V* characteristics were measured at temperatures between 300 and 475 K in the horizontal heating furnace for each specimen (length 200 mm, diameter 4 mm). After the thermal conditions in the furnace were stabilized, a low voltage (-0.02 to $+0.02$ mV) was applied to the ends of the specimen.

Current-voltage (*I-V*) characteristics were obtained by using the Hewlett-Packard HP4140B picoammeter for different temperatures.

During the experiments and at constant temperature, a low voltage (mV) was applied to the ends of the specimen because the cylindrical metallic specimens have very low resistance. Liquid nitrogen and ice-water were used for electrical resistivity measurements of the specimens at temperatures between

100 and 275 K, respectively. Hence, the I - V characteristics of all the specimens have been measured over the temperature range 100-475 K.

The temperature distribution along the specimens was measured by means of three thermocouples (K-type) positioned (not welded) approximately 6 cm apart from each other and perpendicular to the specimen; the furnace temperature was controlled by the temperature controller. Average specimen temperatures were calculated with the temperature values measured by means of these thermocouples.

3. Results and Discussion

Graphs of the I - V characteristics of the specimens obtained by using measurement data are shown in Fig. 2(a)-(d). As can be seen in these figures, the current values are linearly proportional with the voltage values in both directions (forward and reverse), but this ratio decreases as the temperature increases. As can be seen in Fig. 3(a)-(d), the electrical resistivities of the specimens increased with increasing temperature for each alloy system. Electrical resistivity (ρ) gradually increases with increasing temperature up to 350 K but increases rapidly above 350 K. The electrical resistivity versus temperature plots of the specimen Cd-Sn are given in Fig. 3(a), and the resistivity versus temperature plots of Bi-Sn are shown in Fig. 3(b). As can be seen in these figures, the electrical resistivity of Cd-Sn increases from 14.5 to 18.6 $\mu\Omega \cdot \text{cm}$ and that of Bi-Sn increases from 37.6 to 42.6 $\mu\Omega \cdot \text{cm}$ with an increase in temperature. The obtained resistivity ranges are in good agreement with previous work (Ref 18). As can be seen in Fig. 3(c) and (d), the electrical resistivities of the Al-Si eutectic and Al-3wt.%Si hypoeutectic alloys increase from 2.8 to 3.8 $\mu\Omega \cdot \text{cm}$ and from 2.5 to 3.8 $\mu\Omega \cdot \text{cm}$ with an increase in temperature, respectively. The resistivity ranges obtained for these samples are in good agreement with previous work (Ref 18, 19).

The residual resistivity ratio $(\rho - \rho_0)/\rho_0$ as a function of ΔT is shown in Fig. 4, where ρ_0 is the resistivity at 273 K. The figure shows that the residual resistivity ratios increase with increasing ΔT for each alloy system. The behavior of the residual resistivity ratio $(\rho - \rho_0)/\rho_0$ depending on ΔT was also observed in different alloy systems by various researchers (Ref 20-22). The calculated average temperature coefficients of electrical resistivities (α) of the Cd-Sn and Bi-Sn eutectic alloys in the temperature range of 100-450 K were found to be 1.56×10^{-3} and $0.71 \times 10^{-3} \text{ K}^{-1}$, respectively. Similarly, the average α values of the Al-Si eutectic and Al-3wt.%Si hypoeutectic alloys were found to be 1.5×10^{-3} and $2.34 \times 10^{-3} \text{ K}^{-1}$ in the temperature range of 100-475 K, respectively.

4. Conclusions

As a result, the temperature dependence of electrical resistivity and the residual resistivity ratio of Cd-Sn, Bi-Sn, and Al-Si eutectic and Al-3wt.%Si hypoeutectic alloys were investigated. The experimental results obtained for Cd-Sn and Bi-Sn eutectic alloys are in good agreement with previous work (Ref 18). Similarly, the results obtained for Al-Si eutectic and Al-3wt.%Si hypoeutectic alloys are in good agreement with the results in Ref 19.

Acknowledgments

This project was supported by the State Planning Organisation of Turkey (2003K 120880-4). The authors thank the State Planning Organisation of Turkey for their financial support. This work was carried out at Niğde University, Faculty of Art and Science, Department of Physics.

References

1. R. Elliott, *Eutectic Solidification Processing*, Butterworths, London, 1983, p 60-91
2. M.C. Flemings, *Solidification Processing*, McGraw-Hill, New York, 1974, p 67-103
3. W. Kurz and D.J. Fisher, Dendrite Growth in Eutectic Alloys: The Coupled Zone, *Int. Metals Rev.*, 1979, **24**, p 177-204
4. B. Bay, N. Hansen, and B.K. Wilsdorf, Microstructural Evolution in Rolled Aluminium, *Mater. Sci. Eng. A*, 1992, **158**, p 139-146
5. A.M. Rana and M.I. Ansari, The Particle Coarsening in Fe-Cu Alloy, *Mod. Phys. Lett. B*, 1995, **9**(6), p 343-350
6. M.I. Ansari, A.M. Rana, and Z.A. Sheikh, The Formation of Precipitates and G.P. Zones in Fe-Cu Alloys, *Turk. J. Phys.*, 1994, **18**, p 640-647
7. A.M. Rana, A. Qadeer, and T. Abbas, Crystallization Induced Phase Changes in Amorphous Fe₈₄Nb₇B₉ Alloy, *Proc. 6th Int. Symp. Advanced Materials*, M.A. Khan, K. Hussain, and A.Q. Khan, Ed., Dr. A.Q. Khan Research Laboratories, Islamabad, Pakistan, 1999, p 151-154
8. A. Perumal, Critical Behavior of Electrical Resistivity in Amorphous Fe-Zr Alloys, *Pramana J. Phys.*, 2001, **56**(4), p 569-577
9. A. Shamim, M. Suleman, A. Mateen, M. Ahmad, M. Nawaz, and M.S. Zafar, Crystallization and Other Phase-Change Studies of (Fe_{0.8}Ni_{0.2})₇₆B₂₄ Glassy Alloy, Using Resistivity Measurements, *J. Mater. Sci. Lett.*, 1988, **7**(12), p 1313-1314
10. C.A.S. Lima, R. Oliva, G. Cardenas, E.N. Silva, and L.C.M. Miranda, Influence of the Thermal Annealing on the Electrical Resistivity and Thermal Diffusivity of Pd:Ag Nanocomposites, *Mater. Lett.*, 2001, **51**, p 357-362
11. P.J. Wang, Z.Q. Zeng, Z.L. Gui, and L.T. Li, Strontium-Lead Titanate Ceramics with Positive Temperature Coefficient of Resistance, *Mater. Lett.*, 1997, **30**, p 275-277
12. P. Berwian, A. Weimar, and G. Muller, In Situ Resistivity Measurements of Precursor Reactions in the Cu-In-Ga System, *Thin Solid Films*, 2003, **431**, p 41-45
13. M. Kass, C.R. Brooks, D. Falcon, and D. Basak, The Formation of Defects in Fe-Al Alloys, Electrical Resistivity and Specific Heat Measurements, *Intermetallics*, 2002, **10**, p 951-966
14. R.V. Dremov, N. Koblyuk, Y. Mudryk, L. Romaka, and V. Sechovsky, Electrical Resistivity and Magnetism in Some Ternary Intermetallics, *J. Alloys Compd.*, 2001, **317-318**, p 293-296
15. S. Beckman, B.A. Cook, and M. Akinc, Analysis of Electrical Resistivity of Compositions within the Mo-Si-B Ternary System, Part I: Single Phase Compounds, *Mater. Sci. Eng. A*, 2001, **298**, p 120-126
16. E. Çadırılı, A. Ülgen, and M. Gündüz, Directional Solidification of Aluminium-Copper Eutectic Alloy, *Mater. Trans. JIM*, 1999, **40**, p 989-996
17. E. Çadırılı and M. Gündüz, The Dependence of Lamellar Spacing on Growth Rate and Temperature Gradient in the Lead-Tin Eutectic Alloy, *J. Mater. Process. Technol.*, 2000, **97**, p 74-81
18. J. Glazer, Microstructure and Mechanical Properties of Pb-free Solder Alloys for Low-Cost Electronic Assembly: A Review, *J. Electron. Mater.*, 1994, **23**(8), p 693-700
19. Atlas of Microstructures of Industrial Alloys, T. Lyman, Ed., *Metals Handbook*, ASM International, 1972, Vol 7
20. K. Mitsui, Change in Electrical Resistivity during Continuous Heating of Cu₃Pd Alloys Quenched from Various Temperatures, *Philos. Mag. B*, 2001, **81**, p 433-449
21. A.A. Al-Aql, Electrical Resistivity Measurements in Ni-Cr Alloys, *Mater. Des.*, 2003, **24**, p 547-550
22. A.A. El-Daly, A.M. Abdel-Daiem, and M. Yousf, Effect of Isothermal Ageing on the Electrical Resistivity and Microstructure of Pb-Sn-Zn Ternary Alloys, *Mater. Chem. Phys.*, 2002, **78**, p 73-80